PRELIMINARY MEASUREMENT RESULTS OF THE UPGRADED ENERGY BPM AT FLASH

U. Mavrič, M. Felber, Ch. Gerth, H. Schlarb, DESY, Hamburg, Germany
W. Jałmużna, A. Piotrowski, TUL-DMCS, Łódź, Poland

Abstract

The energy beam position monitor in the dispersive section of the two bunch compressors is a valuable instrument for regular operation of FLASH. Recently, an upgrade of the existing instrument to an MTCA form factor has been started. The basic principle of the time-of-flight measurement will remain the same; however the detection of the phases and amplitudes of two pulses has been moved to the programmable gate array. Other changes include different RF frequencies of detection, optimization of the front-end section and integration into the control system. A preliminary version of the system has been tested at FLASH and the results are presented in the paper.

INTRODUCTION

The basic principle of operation and the first implementation of the energy beam position monitor (EBPM) have been presented in Refs. [1-3]. In principle, the position measurements of the EBPM, located in the dispersive section of a bunch compressor, can be used for energy measurements of individual bunch. The dynamics of the bunch compressor play a crucial role in understating the principle of operation of the instrument and are described in Refs. [3,4]. Small displacements Δx of the bunch in the vicinity of the centre of the chicane due to a change of the normalized energy (ΔE/E) can be approximated in first-order transport theory by

$$\Delta x = R_{16}\frac{\Delta E}{E}. \qquad (1)$$

The horizontal dispersion R_{16} in the first bunch compressor BC2 at FLASH can be varied from 284 mm to 358 mm, and it is planned to be in the range of 400 mm to 700 mm in case of the second and third bunch compressor at the European XFEL.

The position of the EBPM is determined indirectly by measuring the phase difference between two pulses coming from the pick-up. The present EBPM pick-up is designed as two independent parallel coaxial lines where the perpendicularly passing beam excites two pulses on each coaxial line that are traveling in the opposite directions (see Fig. 1). By summing the two pulses traveling in the same direction (from the upper and lower rods), the dependence of the measurement on the transverse displacement of the beam is reduced. The length L of the rod is 183 mm (point where the tapering starts – see [1]) meaning that the maximum time difference between pulses can be app. 600 ps. One way of detecting such type of time difference is measuring the phase difference at a known frequency. The phase ambiguity of the measurement is avoided if the measured time difference is small enough in order to correspond to a phase difference that is smaller than period of the RF wave.

In our case, the electronics detects the part of the spectrum close to 1.3 GHz and it measures its phase compared to the global FLASH reference phase (at 1.3 GHz). The maximum phase difference between the two pulses at 1.3 GHz equals to 280º, which still allows for unambiguous detection of the position of the bunches.

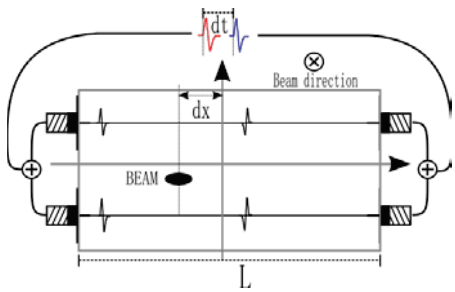

Figure 1: Time of flight principle.

The detected phase difference is used to calculate the horizontal beam position by using the formula:

$$\Delta x = \frac{\Delta\varphi}{2\pi}\cdot\frac{c}{f_0}. \qquad (2)$$

Where c represents the speed of the two signals in the pick-up structure, f0 is the detection frequency (1.3 GHz in this case) and Δφ [rad] is the measured phase difference between the two pulses.

One of the most attractive features this detection scheme of the EBPM is that combines a high dynamic range (over the whole length of 183 mm) and high resolution of the measurements (<20 um). Both, dynamic range and resolution depend on the frequency of detection. The high dynamic range requires a lower frequency due to phase ambiguity. The high resolution requires a higher frequency of detection. This schizophrenic situation may be overcome by having two different frequencies of detection. The low frequency for coarse measurements which allows to track the absolute position within the chicane and the high frequency for fine measurements which allows to precisely measure relative changes of the position. In case all other sub-components operate within their design specifications, the

ISBN 978-3-95450-115-1

resolution of the measurement is ultimately limited by the quality of the analog-to-digital converter (ADC). An average of-the-shelf 16 bit ADC with the sampling frequency in the range of 150 MSPS gives app. a theoretical 6 mº RMS resolution over the whole Nyquist zone bandwidth. According to Eq. (2), this corresponds to app. 4 µm RMS resolution in position at 1.3 GHz frequency. The resolution is inversely proportional with the detection frequency (see Eq. (2)).

SYSTEM OVERVIEW

The system is based on the commercially available digitizer/processing unit SIS8300 [3] designed according to the MTCA.4 standard. The digitizer is composed of five dual-channel ADCs which ship data sampled at 108 MSPS to a Virtex 5 FPGA. The detection scheme uses an analog down-conversion to an intermediate frequency (IF) at app. 36 MHz and a digital amplitude and phase detection. The measured phases are then transmitted through the PCIe bus to the CPU and they are averaged, additionally scaled, subtracted and multiplied with appropriate constants to finally get the position values. The final measurement is composed of two position values (one for each pick-up) for each individual bunch in each RF pulse.

Local Oscillator and Clock Generation

The simplified block diagram of the local oscillator and clock (CLK) generation is shown in Fig. 2. The CLK signal is generated by dividing the REF (1.3 GHz reference) by 12. The LO is generated by dividing one branch of the 1.3 GHz reference by 36 and mixing it up with the other 1.3 GHz branch. The module foresees three different LO signals at 650 MHz, 1336 MHz and at 3322 MHz. The lower LOs are used for course measurements and the higher ones for high resolution measurements.

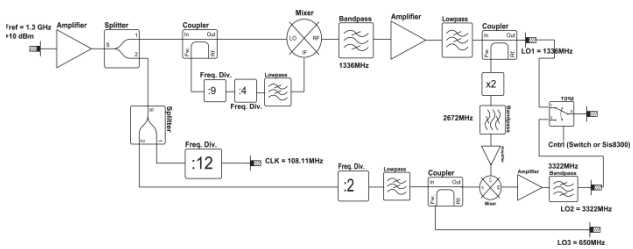

Figure 2: Block diagram of the LO and CLK generation.

Front-End and Down-Converter

The bipolar pulses at the output of the pick-ups have a bandwidth of app. 6 GHz and can be as high as 60 Vpp. The RF front-end is used to properly stretch and attenuate the pulses so that they can be fed into the down-converter. The down-converter module (DWC) has been designed as a rear transition module (RTM) which is part of the MTCA.4 standard configuration. Originally designed for LLRF purposes (see [5]), this 10 channel broadband unit can also be used for many other applications. Fig. 3 shows the block diagram of one such cell of the RF front-end and the down-converter.

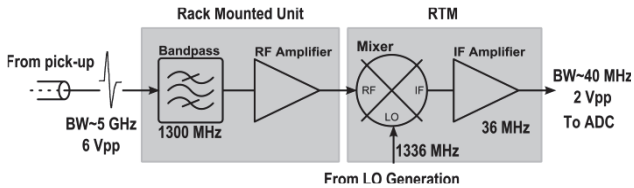

Figure 3: Block diagram of the RF processing chain of the RF front-end and down-converter.

The choice of the RF band-pass filter is critical from the perspective of quality of detection. The optimization parameters of the filter are the bandwidth and placement of the filter poles. A low filter bandwidth allows for a longer duration of a pulse, however, to the expense of lower output amplitude (less integrated power). A non-flat group delay response type of filter (e.g. elliptic or Chebyshef) causes interference patterns in the impulse response of the filter. If the response is too long, it can interfere with the next bunch. It is therefore advisable to use Gaussian or Bessel-type band-pass filters for which the impulse response is of Gaussian-like shape (with no additional lobes). The bandwidth used in our case is app. 100 MHz in order to achieve the full-scale of the ADC (maximum SNR). After down-conversion to the IF, the pulse is stretched to app. 100 ns, which gives app. 11 ADC samples per pulse. These samples can be further averaged which leads to reduction of the bandwidth, therefore improvement of the RMS value of the measurement resolution.

Digitizer and Digital Processing

Fig. 4 shows a simplified block diagram of the DSP structure.

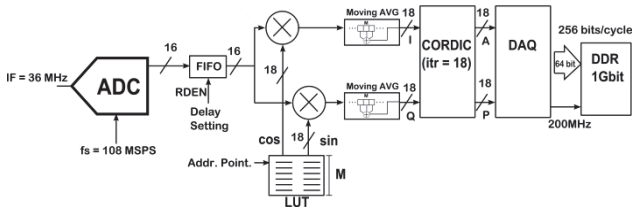

Figure 4: Block diagram of the digital signal processing in the FPGA.

The down-conversion to baseband is achieved by multiplying the sampled signal with sine and cosine values stored in the FPGA RAM. Depending on the ratio between the IF and CLK frequency the length of the look-up-table (LUT) can vary. In order to filter the 2nd harmonic of the IF frequency generated by multiplication, a moving average filter is used. Again, the length of the moving window is defined by the ratio between the IF and the CLK frequency. The baseband I and Q signals are passed to a CORDIC with 18 iteration steps. The obtained amplitude and phase values are then shipped to a DDR RAM which is accessible by the CPU through the PCIe.

MEASUREMENTS

For the preliminary measurements with the EBPM in the first bunch compressor BC2 at FLASH, only one pair of pick-ups was used. A small change in the gradient of the first accelerating module ACC1 was induced, and the beam position was measured. Figure 5 shows the position change as a function of energy change. The blue data points correspond to the normalized measurement and the red curve is the expected normalized change according to the theoretical calculations of the electron bunch trajectory.

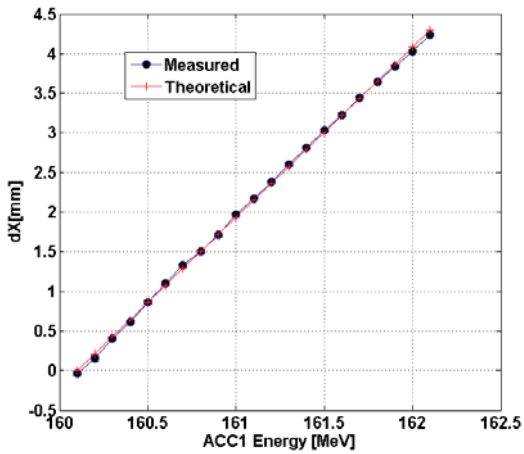

Figure 5: Measured (blue dots) and theoretical (red crosses) position deviation as a function of beam energy change in the centre of the first bunch compressor at FLASH.

In the second set of measurements the resolution of the instrument was determined by correlating two adjacent bunches in a bunch train. It is assumed that disturbances such as beam orbit jitter and energy jitter are the same for both bunches, meaning that a difference of the two position readings includes mainly the disturbances added by the instrument (higher by $\sqrt{2}$). The correlation of the two pulses can also be depicted in Fig. 6 where the position reading of the 2nd bunch is plotted as a function of the 1st one. The correlated disturbance of the two bunches will move the measurement points along the reference line (black line) and the uncorrelated disturbances of the two pulses will cause the measurement points to move perpendicular to the black line. The calculated standard deviation of the uncorrelated part of disturbances equals 20 um which according to Eq. 1 corresponds to $5.6 \cdot 10^{-5}$ energy resolution. For the presented measurement we have not exploited the full working range of the ADCs which gives some head room for resolution improvement.

FUTURE WORK

In order to avoid long-term drifts and repeatability of the system the calibration of the cables and front-end electronics needs to be defined. The latter is particularly important from the perspective of the absolute calibration of the instrument.

For the European XFEL a new pick-up design has been started due to the large vacuum chamber cross-section of 400 mm x 40 mm. The design goal is to achieve 18 GHz bandwidth for beam charges in the range 20 pC to 1 nC.

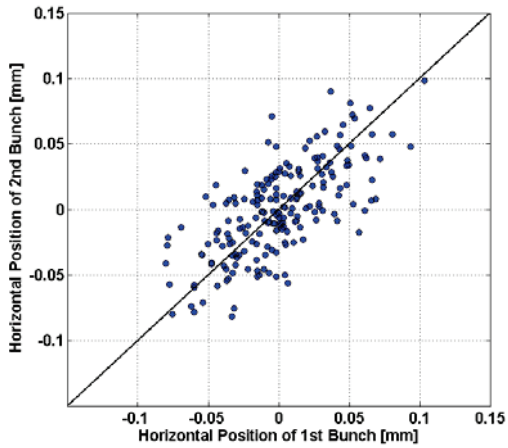

Figure 6: Correlation of horizontal position readings of two adjacent bunches.

CONCLUSIONS

The EBPM instrument has been successfully upgraded from the VME-based to the MTCA-based system. The goal of high data-rate throughput, reliability, maintainability and standardization has therefore been fulfilled as most of the modules, both hardware and software, are based on the standard European XFEL LLRF system. An alternative scheme of down-conversion and quadrature detection has been employed to detect time differences between pulses. The different detection scheme of phase (on IF) has been successfully checked. The measured resolution and sensitivity of a single-rod pick-up are promising and they are still open for improvements.

REFERENCES

[1] K. Hacker et al., "Large Horizontal Aperture BPM and Precision Bunch Arrival Pickup", DIPAC'07, Venice, TUPB20.

[2] K. Hacker et al., "Demonstration of a BPM with 5 Micron Resolution over a 10 cm Range", FEL'09, Liverpool, WEPC70.

[3] K. Hacker, "Measuring the Electron Beam Energy in a Magnetic Bunch Compressor", PhD Thesis, Hamburg, 2012.

[4] P. Castro, "Beam trajectory calculations in bunch compressors of TTF2", Internal DESY technical note.

[5] J. Branlard et al., "The European XFEL LLRF System", this conference, MOOAC01.

ISBN 978-3-95450-115-1